

3D Reconstruction of Human Body in Virtual Fitting Room Based on Kinect

Khadijaha Mansour*

Jawaharlal Nehru University, India

**corresponding author*

Keywords: Virtual Fitting, Kinect Technology, 3D Reconstruction, Augmented Reality

Abstract: With the progress of the times, more and more scientific and technological elements have been integrated into people's daily life, which is manifested in fitting. Virtual fitting technology provides people with a more convenient and interactive fitting mode. The launch of Microsoft Kinect solves the problem of human body spatial information acquisition and facilitates the development of virtual fitting systems. This paper uses modeling software to build a human body 3D clothing model, and focuses on the human body 3D clothing modeling. This paper binds the three-dimensional clothing model with human bones to the user's three-dimensional information collected through the Kinect camera to achieve the fusion of virtual and virtual clothing. This paper simulates the physical characteristics of clothing fabrics to improve the realism of virtual clothing degree. The iterative nearest point algorithm is improved. First, the voxel grid is down-sampled for the two point clouds, and then the scale-invariant feature points of the source point cloud are found and saved as a point cloud. The saved point cloud is registered with the target point cloud sampled from the voxel grid. In this paper, the human body point cloud data is collected through Kinect, and the point cloud segmentation, point cloud registration and point cloud reconstruction are studied separately, which makes the Kinect-based 3D human body modeling method more efficient and accurate. This paper proposes a method of iteratively deforming the standard model using the mesh deformation migration algorithm. The method is to establish a mapping relationship between models by given a set of corresponding point pairs between the source grid and the target grid, and realize the constrained deformation from the source grid to the target grid. Experiments show that the algorithm proposed in this paper uses a cheap depth camera to scan the human body. The algorithm preprocessing time is only about 1 second, and the average optimization time is about 3.6 seconds. It can overcome the shortcomings of low depth camera data accuracy, and the reconstruction time is short and the result is high accuracy.

1. Introduction

The combination of traditional clothing companies and the somatosensory virtual fitting system makes the somatosensory virtual fitting technology gradually enter people's lives. The

somatosensory virtual fitting system can greatly improve the shopping experience of consumers, and at the same time, to a certain extent, it can make up for the shortcomings of traditional physical stores such as inconvenient shopping, high clothing prices, and inability to conduct information statistics, thereby increasing the sales volume of clothing in physical stores. The somatosensory virtual fitting technology has opened up a new path for the development of traditional clothing companies. Three-dimensional human body models have been widely used in virtual fitting, film and television animation, medical research, military education and other fields for a long time. In order to meet the needs of three-dimensional human models in various aspects, it is especially important to simulate three-dimensional models with personalized appearances according to different individuals. important.

There are many methods for 3D human body modeling in academic research. The most common method is to obtain human body model data through modeling software or 3D scanner to obtain different parameterized human body models. In foreign countries, Figueroa N uses a method based on Kinect human body reconstruction. This method first uses three Kinects to obtain human body surface data, and then uses image feature points to perform local registration on the scanned data, and then optimizes the registered model globally. This method has high practicability, and the device acquires human body surface data quickly, but it has the disadvantages of low quality of the depth data initially acquired by the Kinect device, resulting in low registration accuracy and inconvenient carrying of the fixed device [1]. Boonbrahm P uses the Kinect device to scan the human body for a week to obtain the depth data information of the human body surface, firstly generate a point cloud of the human body surface, and then use Pro/E software to reconstruct the human body model [2]. PMok K W uses a Kinect to model the human body, and proposes a method to obtain a three-dimensional human body model from the noisy monocular RGB image and the rougher depth image obtained by the Kinect device [3].

In China, Wan Y uses the method of combining color information and depth information to reconstruct a complete three-dimensional human body model. This method needs to register the data obtained from scanning at various angles to reconstruct the three-dimensional human body model [4]. J Sun proposed a Kinect-based method to quickly reconstruct a three-dimensional human body model. This method uses 4 Kinect devices to scan the human body from various angles, denoise the obtained point cloud and reconstruct the human body, using the standard model in the SCAPE human body model library. Parameterized fitting deformation to obtain a three-dimensional human body model with a smooth surface [5]. Liu, Zhenbao proposed a method to complete 3D human body modeling through depth data obtained by Kinect equipment. This method can obtain experimental data faster, but does not perform noise processing on the acquired depth images, and uses computer hardware in the experiment the requirements are high, and GPU accelerators are required, which increases the experimental overhead [6].

This paper introduces the SIFT algorithm and the ICP algorithm, and combines the SIFT feature points to improve the ICP algorithm, which improves the speed and accuracy of the algorithm. Furthermore, the transformation matrix in the registration process is explained and a registration is proposed. The method of two point clouds with a poor initial position.

2. Research on 3D Reconstruction of Human Body in Virtual Fitting Room Based on Kinect

2.1. The Design of Human Body Modeling in 3D Clothing Virtual Fitting

The 3D clothing virtual fitting system is designed to meet the trend of personalized production. It uses clothing technology to generate models for 3D models and 3D clothing objects, and uses visual technology to extract the model's body data; users can see the 3D on the computer screen. The clothes are worn on mannequins synthesized according to their own size, as if they were standing in

front of a mirror [7-8]. Therefore, the three-dimensional clothing virtual fitting system must first have a real body shape that can reflect the wearer, and then perform three-dimensional dressing on this basis, using three-dimensional clothing effect simulation technology to show various overall effects after dressing; digital display of the degree of clothing fit, According to the degree of fit, it can be decided whether or not it needs to be modified and where it needs to be modified until the consumer is satisfied.

(1) Key classes used in 3D human modeling

The 3D human body model reconstruction sub-module program is implemented by calling OpenGL programming in the Visual C++ environment, using single document/view mode, over-class construction and operation, to realize the reconstruction of the human body model and related operations [9]. In the document view structure of VC++, the application data is stored in the document class object as member variables, and the visual object accesses the member variables of the document class through pointers. One of the main tasks of the document class is to manage the data disk access of the document. The key function to achieve disk access in the document class is the `CDocument::Serialize ()` function. The word `Serialize` can be interpreted as "serialization" on the surface. The concept of transformation actually means that an object can store its current state in continuous storage media, and restore its state when needed [10-11]. In specific applications, you need to reload the `CDocument::Serialize ()` function, and call the `CWinApp::OnFileOpen ()` function in the message response function of the Open command of the File menu to automatically call the `CDocument::Serialize ()` function to implement the document Read. Here is a brief introduction to some main classes:

- 1) `C3DSObject` class. Describe the data structure of the 3D human body model.
- 2) `C3DSReader` class. It is used to read and process files.
- 3) `CtriObject` class. Complete the drawing of the human body model.
- 4) `3DModel` class. This class is the core of the entire program. It is used to store and manipulate the related information of the entire scene. It includes the linked list header information of `C3DSObject`, `tMaterial`, `tLight` and some other classes. Operate the relevant information in the scene by operating the corresponding linked list [12].
- 5) `DModelDoc` class. This class inherits the `Cdocument` and `3DModel` classes. It is the document of the entire application and the data object processed by the user.

(2) Kinect somatosensory technology

Taking into account the possibility of occlusion or overlap between various parts of the human body, the developers of Kinect used the depth data of the front, side and top of the human body to perform machine learning, and finally calculated the position of each bone node of the human body [13].

The corresponding steps from left to right are:

- 1) Use the depth image of the human body to separate the human body from the background;
- 2) Identify various parts of the human body and mark them in different colors;
- 3) Taking into account the possibility of occlusion or overlap between various parts of the human body, the depth data of the three angles of the front, side and top of the human body are used for machine learning, and finally the position of each bone node of the human body is calculated [14]. Skeleton tracking is the basis of Kinect's somatosensory operation. Kinect uses bone tracking to create a "digital skeleton" of the user's body. When the human body moves to the left or right or even jumps, the "digital skeleton" of the user's body will keep the same movement as the human body. It's like looking in a mirror [15]. The degree of matching between the "digital skeleton" and the real human body determines the performance of bone tracking, and the degree of matching depends on the number of bone nodes that Kinect can obtain in real time.

2.2. Point Cloud Registration Method Based on SIFT Feature Points

(1) Downsampling of voxel grid

Since the number of point clouds in the obtained point cloud data is relatively large, it will take a lot of time if all are used for experiments, so some point clouds are used to replace all point clouds to improve the experiment speed [16-17]. The VoxelGrid class in PCL can achieve this purpose. It creates a three-dimensional voxel grid from the input point cloud data (think of the voxel grid as a collection of tiny spatial three-dimensional cubes), and then uses it in each voxel the center of gravity approximates the other points in the voxel. Proceed as follows:

1) Determine the side length L of the cube. The determination of L is very critical. If L is too large, the search efficiency will be reduced. If L is too small, many empty grids will appear. The side length of the small cube grid is:

$$L = a^3s/c(1)$$

Among them, a is the scale factor used to adjust the side length of the small cube grid, s is the scale factor, and c is the number of point clouds in the small grid.

2) The volume of the three-dimensional voxel grid is:

$$V = L_xL_yL_z(2)$$

Among them, L_x , L_y , and L_z are the maximum ranges of the point cloud on the x , y , and z axes, respectively. The number of point clouds contained in the unit small grid is (N is the total number of point clouds in the point cloud data):

(2) SIFT algorithm

The SIFT algorithm is an algorithm for describing local features of an image based on scale space. Although it can only describe the local features of the image, the feature remains stable to noise, affine transformation, and viewing angle changes, and remains invariant to brightness changes, scale scaling, and rotation. The steps of SIFT feature point detection are as follows:

The convolution of the original image $I(x, y)$ and the Gaussian kernel $G(x, y, \sigma)$ is defined as the scale space $L(x, y, \sigma)$ of an image:

$$L(x, y, \sigma) = G(x, y, \sigma) \otimes I(x, y)(3)$$

Among them, σ is the scale space factor that determines the degree of image smoothness, (x, y) is the pixel coordinates of the image, and $G(x, y, \sigma)$ is the scale variable Gaussian function:

$$G(x, y, \sigma) = \frac{1}{2\pi\sigma^2} e^{-(x^2+y^2)/2\sigma^2} (4)$$

(3) RANSAC algorithm

The RANSAC algorithm is a random parameter estimation method. Its basic principle is to solve the mathematical model parameters that most samples can satisfy through the strategy of sampling and verification. The specific steps are:

1) Choose 4 pairs of matching points from the sample set as the interior point set, and use the minimum variance estimation algorithm to calculate the model parameters for this set;

2) All other matching points are tested with the model obtained in 1), and if they are less than the set threshold, they are added to the interior point set;

3) If the number of iterations is greater than the set threshold, exit; otherwise, repeat steps 1) and 2), select the group with the largest number of interior points as the qualified matching point set, and re-estimate through the new interior point set Model [18-19].

(4) ICP algorithm

The basic principle of the ICP algorithm is to find the corresponding point pairs between the source point cloud and the target point cloud through continuous iteration and solve the transformation relationship until the solved rotation matrix R and translation vector T satisfy the optimal matching under certain conditions [20]. Suppose the two point clouds to be matched are P and Q , and P is the source point cloud:

$$P = \{p_i | p_i \in R^3, i = 1, 2, \dots, N\} (5)$$

Q is the target point cloud:

$$Q = \{q_j | q_j \in R^3, j = 1, 2, \dots, M\} (6)$$

Proceed as follows:

- 1) Set the threshold $\gamma > 0$ and the number of iterations to determine whether the iteration is terminated;
- 2) Find the nearest point p'_i of each point p_i of the source point cloud P in the target point cloud Q;
- 3) Calculate the rigid body transformation matrix R and T of the source point cloud and the target point cloud;
- 4) Update the source point cloud P and calculate $p' = Rp_i + T$;
- 5) Calculate the mean square error:

$$d_{m+1} = \frac{1}{N} \sum_{i=1}^N R_{m+1} p_i + T_{m+1} - p'_i (7)$$

However, with the continuous development and advancement of 3D scanning technology, the point cloud data obtained is getting larger and larger, which causes inconvenience to subsequent experiments. The classic ICP point cloud registration algorithm is not efficient in calculation and takes time. There are many, so this article first performs voxel grid downsampling on two point clouds, reduces the running time by reducing the number of point clouds, and secondly uses the SIFT feature points of the source point cloud and the target point after the voxel grid downsampling. The cloud is registered, and the RANSAC algorithm is used to remove the wrong matching point pairs. In order to improve the accuracy of the registration, the source point cloud is retained after transformation estimation [21-22].

2.3. Kinect Fusion Real-Time Reconstruction Principle

Kinect Fusion real-time 3D reconstruction algorithm realizes 3D reconstruction by matching, positioning and fusing the depth data collected by the Kinect depth camera. Kinect Fusion's real-time 3D reconstruction process is:

- (1) The Kinect device scans the human body to obtain the original depth image, converts the original depth image into a three-dimensional point cloud and calculates the normal vector of each point to obtain the three-dimensional coordinates and normal vector of the point cloud vertex;
- (2) ICP registration of the point cloud with normal vector obtained in the previous step and the predicted 3D point cloud generated by the existing model, the camera position of the current frame can be obtained through calculation;
- (3) According to the camera position of the current frame, use the TSDF point cloud fusion algorithm to fuse the 3D point cloud of the current frame into the existing mesh model;
- (4) Then use the ray projection algorithm to project the point cloud in the current frame from the model projection according to the camera position of the current frame, and then calculate the normal vector of the point cloud to register the input image of the next frame [23-24].

Repeat the above process in this way, by moving the Kinect depth camera to obtain the point cloud of the human body under different viewing angles, a complete three-dimensional human body surface will be initially reconstructed. ICP positioning in Kinect Fusion [32] is to match the 3D point cloud in the current frame with the predicted 3D point cloud. The implementation steps are as follows:

- (5) Determine the corresponding point relationship. A two-dimensional ICP can be used to represent the process. The Kinect device samples and predicts the scanned object at two consecutive positions. First, the point cloud at this moment and the point cloud at the previous moment are simultaneously converted to the camera coordinates of the current frame. Then project to the image

plane through the center of the camera, and the corresponding points are the projection points on the same image plane in the two point clouds. In this process, the Euclidean distance between the corresponding points and the normal vector angle are used to determine Filter the corresponding points.

(6) Camera tracking. Use the GPU-based ICP algorithm to register the point cloud data of the current frame and the point cloud data of the previous frame to obtain the position and direction of the current Kinect camera; use the point-to-plane error to measure the accuracy of the current relative position and direction. In the case of two-dimensional coordinates, the error between points is the tangent distance between them [25]. The relative position is obtained after optimization.

(7) Cube fusion, according to the position and direction of the current Kinect camera, the currently obtained vertices can be transformed into the global coordinate system, and the value of the corresponding small cube (voxel) can be updated, and the linearization method will be used to optimize the problem Transform into a least squares optimization, and calculate the optimal solution by calculating a linear equation system, iterate steps (5) (6) ten times.

(8) Light projection, the light is projected onto the cube, and a rendered visual image of the cube can be obtained. When moving the Kinect device, the Kinect device scans the surface of the object from different perspectives, so that the data in the cube is continuously improved, so that any holes that are not visible in the original image will be filled.

2.4. Image Data Acquisition Preprocessing

(1) Denoising of depth image

To remove noise through a filter, the commonly used method is to treat the depth image as an ordinary image and directly use the image denoising algorithm. A better method is to combine the color image and the depth image to remove the noise of the depth image.

(2) Human body reconstruction of color images

This type of method either uses a collection of images of the same person or estimates the body shape and posture parameters from a single image. Although the input data is not the same, they basically segment the person from the image, and then use the contour or shadow of the human body on the image to estimate body shape parameters.

(3) 3D human body reconstruction from depth camera

The advantage of the depth camera is that it can output point cloud information, so that the reconstruction of the three-dimensional human body model does not depend entirely on the image. The 3D human body reconstruction system proposed in this paper uses 4 Kinects to scan the human body simultaneously from different perspectives. The user only needs to stand in front of the Kinect for a few seconds to complete the scanning process. The obtained point cloud of the human body is first subjected to denoising processing. Here, the multi-frame summation average and bilateral filter [21] are used to remove the noise generated during the scanning process. The denoised point cloud is used as the input of the variable model fitting algorithm, using the SCAPE model and ICP to gradually deform a standard model to the scanned human point cloud.

3. Experimental Research on Human Body 3D Reconstruction Technology in Virtual Fitting Room Based on Kinect

3.1. Exercise Data Extraction

In this system, the user's control of the three-dimensional clothing is finally realized, so that the three-dimensional virtual clothing can follow the user and respond accordingly. To achieve this process, it is necessary to obtain real-time position information and motion information of the user's

bone joint points, including bone point positioning, bone tracking, and motion smoothing operations.

Kinect, the somatosensory device, calculates the depth value of each pixel based on the principle of infrared light reflection. The depth value includes the shape of the target object and the index information of each pixel, and then matches the different positions of the human body through these different shapes in the depth value., and calculate the position information of the joint points at the same time. It can identify objects similar to "big" characters, and can perform background separation, denoising, and feature point classification on the depth pixel value of the object to obtain the user's profile.

3.2. Extraction of Corresponding Points in the Data Set

Register the point cloud X and Y through the ICP algorithm, and get that each point X (x_i) on the point cloud X has the closest point Y (y_k) in the target point cloud Y, and the closest point pair is recorded as $S(x_i, y_k)$. Set the logarithm of the corresponding point pair to be selected. In the second chapter, the source 3D human body model similar to the target model is selected, so the two models are highly similar in height and body circumference, so the registration is completed. In the case of, the selected corresponding point pairs hardly have corresponding errors, and these point pairs are evenly distributed on the three-dimensional human point cloud model to ensure the accuracy of subsequent deformation constraints. Filter the set $S(x_i, y_k)$ to eliminate inaccurate or wrong point pairs, where the conditions are met: the distance between the point pairs is less than 3cm; the line between the point pairs and the vertex normal vector on the point cloud Y. The included angle cannot be greater than 15°, there is only one closest point in X for a point on the point cloud Y, and vice versa. The set $M(x_i, y_k)$ is the closest corresponding point between the filtered X and Y.

3.3. Three-Dimensional Clothing Matching

Since the two-dimensional clothing only binds the user's spine joint points, the clothing can only achieve translational motion, and the clothing has poor follow-up. In the three-dimensional virtual fitting system, three-dimensional clothing can be bound to all the relevant nodes of the user, and the user can control the clothing from various directions, which can achieve a good fitting effect.

In order to enable the deformation of the virtual clothing to be the same as the user's fitting action, human bones are added to each completed 3D clothing model, and then the skinning and weighting of each clothing model is repeated. Assign until the clothing's authenticity effect is optimal. After completing this step, import the 3D clothing model in FBX format into Unity3d software, and render the 3D virtual clothing. It should be noted that the bones of the model cannot be brought into the pipeline during the import process, otherwise the bones of the model cannot be hidden.

4. Experimental Research and Analysis of Human Body 3D Reconstruction in Virtual Fitting Room Based on Kinect

4.1 Image Analysis

In this paper, 30 different images are selected to conduct experiments on different situations. Some of the experimental results are shown below. The above is the original algorithm operation result, and the improved algorithm operation result is shown in Table 1.

Table 1. Image matching data comparison

	Original algorithm matching points	Improved algorithm matching points	Correct rate of original algorithm	Improved algorithm accuracy	Original algorithm takes time/ms	Improved algorithm time/ms
Pan	257	185	0.7653	0.6582	10764	10725
Spin	87	68	0.5975	0.5691	6281	5509
Zoom	329	325	0.8752	0.7794	15728	15859

As shown in Table 1, it can be seen that although the proposed improved algorithm can increase the speed of image matching, it reduces the accuracy of matching. Therefore, the algorithm needs to be further improved in future work so that it does not reduce the matching while increasing the running speed. Correct rate.

4.2. Reconstruction of Three-Dimensional Human Body Model to Realize Virtual Fitting

This article uses ICP to find the corresponding point pairs. This method is overly dependent on the initial position and has no geometric feature constraints. The ICP search results cannot be guaranteed to be completely correct. The human body database used in this article is relatively small and this database collects European human body models. Considering the differences in human body shapes between Europeans and Asians, it will also have a certain impact on the experimental results. The experimental results are shown in Figure 1.

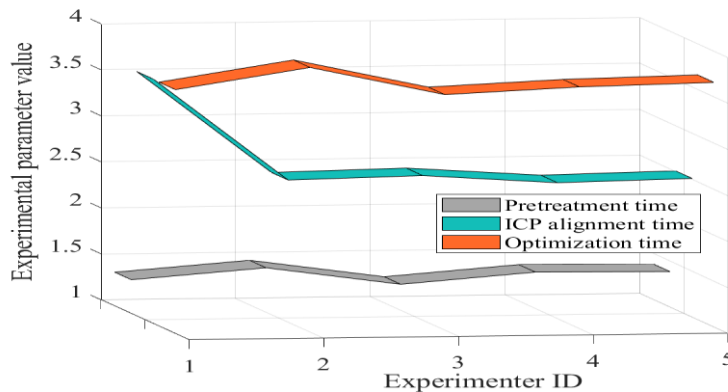


Figure 1. Algorithm time statistics

As can be seen in Figure 1, the algorithm proposed in this paper uses a cheap depth camera to scan the human body. The algorithm preprocessing time is only about 1 second, and the optimization time is about 3.6 seconds on average. It can overcome the shortcomings of low depth camera data accuracy and reconstruction time. Short results have high accuracy. The reconstructed three-dimensional human body model can meet applications in fields such as virtual fitting, and because of the low cost of system hardware, the algorithm proposed in this paper is easy to be popularized and used.

4.3. Experimental Analysis of the Time Required to Reconstruct the Model

In the experiment, 4 experimenters with different body types were selected. Compared with the traditional method, the time efficiency of the method used in this paper is significantly improved. This article only takes less than 1 minute. In addition, the traditional method does not search for similar models in the model library, so that the correspondence between the large-scale standard model and the target model in the reconstruction is not accurate, and the reconstruction takes a long time. The time required for the reconstruction of the three-dimensional human body model for

different experimenters is shown in Figure 2.

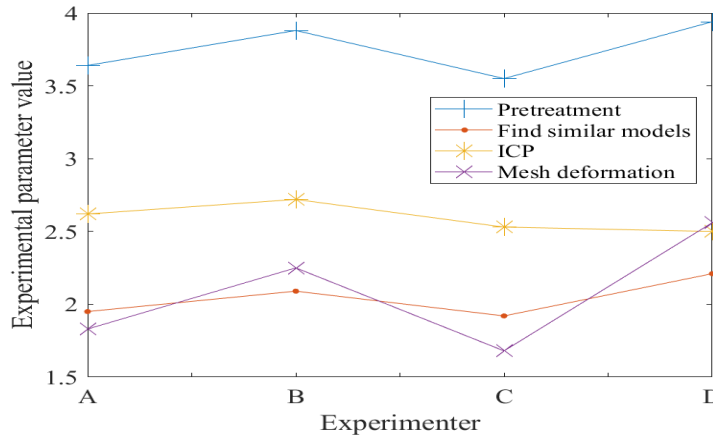


Figure 2. Rebuild time

As shown in Figure 2, this paper obtains a high-precision deformed grid with a height close to the target grid by calculating the optimized energy function. Finally, the comparative analysis of experimental results and experiments in reconstruction error and running time proves that the method used in this paper has obvious advantages in reconstruction time and reduction of reconstruction error compared with other methods.

4.4. Recognition of Human Body Model Features and Calculation of Size

Based on the actual situation and characteristics of the model used in the experiment, this paper selects four characteristics of shoulder width, chest circumference, waist circumference and upper body length for preliminary measurement. Before measurement, we must first identify and locate these characteristic parts, and obtain the profile curve of the cross section of the characteristic part of the model. The experimental results are shown in Figure 3.

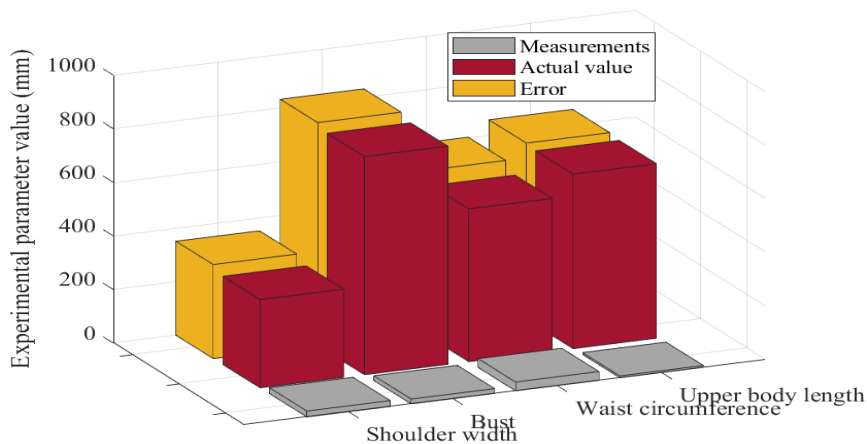


Figure 3. Comparison of some features

It can be seen from the comparison result that there is a certain degree of error between the measured value and the actual value. The main reasons for the error are as follows: Suppose the measurement error of the Kinect device itself. When obtaining the segmented point cloud data of the human body, the process of moving the model is manual operation, and deviations will inevitably occur. During the splicing process of the point cloud, the holes caused by the detected

dead corners were repaired. The actual measured feature position may not exactly match the acquired contour line. For example, when the waist circumference is measured, the tape measure does not necessarily fall on the narrowest part of the model's chest.

4.5. Virtual Clothing Grid Optimization

For clothing mesh models, due to the difference in production technology and standards, the final number of triangular meshes will be different, but too many or too few meshes will affect the final performance: when there are too many meshes, The model will occupy more storage space, consume more processing time, and reduce the overall frame rate; when the number of model meshes is insufficient, the display effect of arcs and curved surfaces is poor, and at the same time, fewer vertices have the effect of subsequent particle posture correction. The impact is serious, and the experimental results are shown in Figure 4.

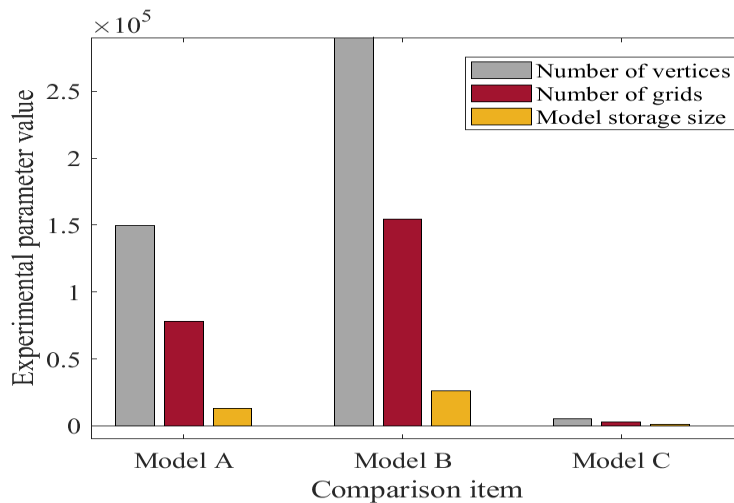


Figure 4. Comparison of Stanford Bunny model under three grid numbers

Taking a three-dimensional human body mesh model as an example, Figure 4 shows the comparison of the rendering effect of the model under different mesh numbers, comparing the space storage of the mesh number occupied by each model, and the difference in processing time, considering the result of multiple storage formats. The size difference is unified into the PLY (Polygon File Format) format. Because the actual model processing operations are diverse, only the model import time under the OpenGL tool is compared here.

5. Conclusion

The 3D human body reconstruction algorithm proposed in this paper uses 4 Kinects to scan the human body from 4 perspectives at the same time, which can avoid the non-rigid deformation of the human body during the scanning process, and can quickly collect data. By calibrating Kinect in pairs, 4 parts of data can be automatically spliced into a whole. Take the collected point cloud as input, find and fit the input point cloud through the SCAPE model and the nearest point of ICP to reconstruct an accurate three-dimensional human body model. This paper proposes a 3D human body reconstruction algorithm based on depth camera. In this paper, four Kinect depth cameras are used to collect data, which can improve the accuracy of the scanned data and shorten the scanning time, and avoid the non-rigid changes of the human body that may occur during the scanning process.

In the chapter of SIFT algorithm research, this paper has deeply studied the SIFT algorithm and improved the algorithm. The main work is to simplify the descriptor of the SIFT algorithm, and

reduce the dimension of the 128-dimensional descriptor in the original algorithm to 12 dimensions, thereby improving the speed of the algorithm. This paper gives the software design of the virtual fitting system and studies the SIFT algorithm. Because of the limited personal level, there are still many shortcomings, which can be improved in the future.

The simulation effect of the virtual fitting interface needs to be further optimized. This system uses 3ds Max for modeling and imports it into the virtual interactive platform built by Unity3d. There is no lighting effect, which reduces the authenticity of the system. Therefore, the interactive interface needs to be further optimized. In the 3D clothing modeling part, the clothing model is not optimized. Due to the large amount of calculation, there is a delay in the operation of the entire system. Therefore, the optimization algorithm is used to optimize the model to shorten the time delay of time replacement. This virtual fitting system can only meet the fitting experience of one user. In future research and development, multiple people can try on garments and gradually improve the virtual fitting system.

References

- [1] Figueroa N , Dong H , Saddik A E . *A Combined Approach Toward Consistent Reconstructions of Indoor Spaces Based on 6D RGB-D Odometry and KinectFusion*. *ACM Transactions on Intelligent Systems and Technology*, 2015, 6(2):1-10.<https://doi.org/10.1145/2629673>
- [2] Boonbrahm P , Kaewrat C , Boonbrahm S . *Realistic Simulation in Virtual Fitting Room Using Physical Properties of Fabrics*. *Procedia Computer Science*, 2015, 7(5):12-16.<https://doi.org/10.1016/j.procs.2015.12.189>
- [3] PMok K W , Wong C T , Choi S K , et al. *Design and Development of Virtual Dressing Room System Based on Kinect*. *International Journal of Information Technology and Computer Science*, 2018, 10(9):39-46.<https://doi.org/10.5815/ijitcs.2018.09.05>
- [4] Wan Y , Lu J , Li A Q . *Registration of 3D Point Cloud of Human Body Based on the Range Images and RGB Images*. *Applied Mechanics & Materials*, 2015, 9(5):656-661.<https://doi.org/10.4028/www.scientific.net/AMM.738-739.656>
- [5] J Sun, T Wang, Z D Li. *Reconstruction of Vehicle-human Crash Accident and Injury Analysis Based on 3D Laser Scanning, Multi-rigid-body Reconstruction and Optimized Genetic Algorithm*. *Journal of Forensic Medicine*, 2017, 33(6):575-582.
- [6] Liu, Zhenbao, Huang, Jinxin, Bu, Shuhui. *Template Deformation-Based 3-D Reconstruction of Full Human Body Scans From Low-Cost Depth Cameras*. *IEEE Transactions on Cybernetics*, 2016:1-14.<https://doi.org/10.1109/TCYB.2016.2524406>
- [7] Park H , Park J , Kim H , et al. *Virtual Dress-Fitting Media Art System using Kinect and Augmented Reality*. *Techart Journal of Arts & Imaging ence*, 2017, 4(2):10-12.<https://doi.org/10.15323/techart.2017.05.4.2.10>
- [8] Liu Z , Huang J , Bu S , et al. *Template Deformation-Based 3-D Reconstruction of Full Human Body Scans From Low-Cost Depth Cameras*. *IEEE Transactions On Cybernetics*, 2017, 47(3):695-708.<https://doi.org/10.1109/TCYB.2016.2524406>
- [9] Ebner T , Feldmann I , Renault S , et al. *Multi - view reconstruction of dynamic real - world objects and their integration in augmented and virtual reality applications*. *Journal of the Society for Information Display*, 2017, 25(3):151-157.<https://doi.org/10.1002/jsid.538>
- [10] Chhaya M P , Melchels F P W , Holzapfel B M , et al. *Sustained regeneration of high-volume adipose tissue for breast reconstruction using computer aided design and biomanufacturing*. *Biomaterials*, 2015, 52(5):551-560.<https://doi.org/10.1016/j.biomaterials.2015.01.025>
- [11] D.-Y. Lü, Huang Z P , Tao G H , et al. *Dynamic Bayesian Network model based golf swing 3D reconstruction using simple depth imaging device*. *Journal of Electronics & Information*

Technology, 2015, 31(5):163-192.

[12] Yoon B , Choi K , Ra M , et al. Real-time Full-view 3D Human Reconstruction using Multiple RGB-D Cameras. *Transactions on Smart Processing & Computing*, 2015, 4(4):224-230.<https://doi.org/10.5573/IEIESPC.2015.4.4.224>

[13] Hu P P , Li D , Wu G , et al. Personalized 3D mannequin reconstruction based on 3D scanning. *International Journal of Clothing Science and Technology*, 2018, 30(2):159-174.<https://doi.org/10.1108/IJCST-05-2017-0067>

[14] Takahashi K , Sakaguchi T , Ohya J . Remarks on a real-time, noncontact, nonwear, 3D human body posture estimation method. *Systems & Computers in Japan*, 2015, 31(14):1-10.[https://doi.org/10.1002/1520-684X\(200012\)31:14<1::AID-SCJ1>3.0.CO;2-0](https://doi.org/10.1002/1520-684X(200012)31:14<1::AID-SCJ1>3.0.CO;2-0)

[15] Barbeito A , Painho M , Cabral P , et al. Beyond Digital Human Body Atlases: Segmenting an Integrated 3D Topological Model of the Human Body. *International Journal of E-Health and Medical Communications (IJEHMC)*, 2017, 8(1):19-36.<https://doi.org/10.4018/IJEHMC.2017010102>

[16] Khan D , Shirazi M A , Kim M Y . Single shot laser speckle based 3D acquisition system for medical applications. *Optics & Lasers in Engineering*, 2018, 105(JUN.):43-53.<https://doi.org/10.1016/j.optlaseng.2018.01.001>

[17] Xu H , Li J , Lu G , et al. Modeling 3D Human Body with a Smart Vest. *Computers & Graphics*, 2018, 75(OCT.):44-58.<https://doi.org/10.1016/j.cag.2018.07.005>

[18] Liu Z , Sun H , Jin G , et al. Study of the Airflow Patterns and of the Characteristics of Bio-Aerosol Nanoparticle Deposition in Human Upper Respiratory Tracts Based on Computed Tomography Scanning Reconstruction. *Journal of Advanced Materials*, 2016, 8(5):987-996.<https://doi.org/10.1166/sam.2016.2654>

[19] Zhu H , Liu Y , Fan J , et al. Video-Based Outdoor Human Reconstruction. *IEEE Transactions on Circuits and Systems for Video Technology*, 2017, 27(4):760-770.<https://doi.org/10.1109/TCSVT.2016.2596118>

[20] Xie L , Zhang X , Xu Y , et al. SkeletonFusion: Reconstruction and tracking of human body in real-time. *Optics and Lasers in Engineering*, 2018, 110(NOV.):80-88.<https://doi.org/10.1016/j.optlaseng.2018.05.011>

[21] Mao A , Zhang H W , Liu Y , et al. Easy and Fast Reconstruction of a 3D Avatar with an RGB-D Sensor. *Sensors*, 2017, 17(5):1113-1124.<https://doi.org/10.3390/s17051113>

[22] Vassilevski Y V , Danilov A A , Gamilov T M , et al. Patient-specific anatomical models in human physiology. *Russian Journal of Numerical Analysis and Mathematical Modelling*, 2015, 30(3):185-201.<https://doi.org/10.1515/rnam-2015-0017>

[23] Sekhavat Y A . Privacy Preserving Cloth Try-On Using Mobile Augmented Reality. *IEEE Transactions on Multimedia*, 2017, 19(5):1041-1049.<https://doi.org/10.1109/TMM.2016.2639380>

[24] Hendrawan Y F , Wahyuningrum R T , Siradjuddin I A , et al. Virtual Fitting Room Mobile Application for Madura Batik Clothes. *Advanced Science Letters*, 2016, 22(7):1783-1786.<https://doi.org/10.1166/asl.2016.7043>

[25] Wang M , Yu C , Fang F . Consumer awareness and function requirement of three-dimensional virtual fitting. *Wool Textile Journal*, 2017, 45(11):78-83.